 ©2002 Kvantovaya Elektronika and Turpion Ltd

PACS numbers: 42.55.Lt; 42.60.Lh
DOI: 10.1070/QE2002v032n08ABEH002269

Xe laser pumped by fast electrons generated in a barrier discharge

A.V. Azarov, S.V. Mit'ko, V.N. Ochkin

***Abstract*. A compact pulsed generator of a kiloelectronvolt electron beam based on an open barrier discharge in a dense gas is proposed and developed. A stable discharge was observed in the experimental setup in a broad range of pressures up to the atmospheric pressure. At moderate pressures of the gas ($\sim 5 - 20$ Torr), the efficient generation of an electron beam was observed with a current density of ~ 1 A cm^{-2} and the discharge area of ~ 100 cm^2. The electron energy was $\sim 2 - 10$ keV. The pulse repetition rate could be varied from 10 Hz to 10 kHz without changing the electron-beam parameters. By injecting an electron beam into a neutral gas, lasing was obtained at the transitions of a Xe atom in the 2-μm region with an output power of ~ 0.22 mW kHz^{-1}.**

Keywords: *electron-beam-pumped laser, open electron-beam generator*.

1. Introduction

It is profitable to use in some plasma technologies the electrons with energies exceeding the average electron energy in a self-sustained discharge. This is especially important in the case of high densities of a gas producing plasma for providing the homogeneity and stability of the medium and efficient excitation of the electronic states and ionisation of particles.

Two methods for generating fast electrons have been discussed in the literature. In the first (electroionisation) method, an electron beam formed in a vacuum electron gun is injected into a gas through a separating foil [1, 2]. In the second (open discharge) method, an electron beam is generated directly in the open discharge of a working gas between a metal cathode and a closely spaced (less than 1 mm) perforated anode [3 – 5].

As a rule, an electron gun produces $\sim 100 - 200$-keV electron beams. Although such high energies are not directly required for achieving the aims mentioned above, it is expedient to use them to excite the large volumes of dense gases, when a large mean free path of electrons is important. The advantages of such beams are manifested when it is necessary to inject them through a foil, which, as a rule, is weakly transparent for lower-energy electrons. However, if the extension of a medium is relatively small, then the latter circumstance becomes an unjustified technological restriction, which stimulates the search for materials for separating elements that would be more transparent for low-energy electrons. A recent achievement in this field is paper [6], where a ceramic membrane made of silicon nitride of thickness 300 nm absorbing less than 10 % of 10-keV electrons was described. Such a membrane of width 0.7 mm and length 40 mm withstands a pressure drop up to 2 atm. The average beam current did not exceed, however, 5 mA cm^{-2}, which was caused by the membrane damage upon heating.

The open discharge method has been studied less thoroughly than the electroionisation method. This method provides $1 - 10$-keV electron beams with a current density of $1 - 100$ A cm^{-2}. However, the stability region of an open discharge is limited by low pressures of a working gas. The highest limiting pressure was observed for helium and was ~ 20 Torr in a continuous regime and ~ 100 Torr in a pulsed regime (see also [7, 8]). At higher pressures (or at higher applied voltages), the discharge transforms to an arc. In our opinion, these limitations are caused by a high conductivity of a metal cathode. A fluctuation increase in the local conductivity in the vicinity of some point near the cathode surface (microbreakdown of the cathode layer) reduces the potential of the entire surface, resulting in the development of instability.

To solve this problem, we studied in this paper the pulsed generation of an electron beam in a barrier discharge, whose electrode system consists of the successively arranged metal cathode, dielectric (barrier), and perforated metal anode. We verified the efficiency of our setup by studying lasing at the $5d[3/2]_1^o - 6p[3/2]_1$ ($\lambda = 2.03$ μm) and $5d[3/2]_1^o - 6p[1/2]_0$ (2.65 μm) transitions in atomic xenon. We have chosen xenon for our experiments because, according to the model proposed in paper [9], the population inversion in xenon is produced due to three-body collisions and electron – ion recombination, which requires the efficient ionisation in a high-density gas.

In paper [10], dielectric barriers located between a cathode and a grid anode also stabilise the discharge. However, a substantial difference of an electron-beam generator proposed by us in this paper is that a dielectric not only stabilises the discharge but also is a source of electrons, thereby removing the limitation imposed on the minimal electron energy required to overcome a barrier.

A.V. Azarov, S.V. Mit'ko, V.N. Ochkin P.N. Lebedev Physics Institute, Russian Academy of Sciences, Leninskii prosp. 53, 119991 Moscow, Russia; http://www.lebedev.ru

Received 26 March 2002
Kvantovaya Elektronika **32** (8) 675 – 679 (2002)
Translated by M.N. Sapozhnikov

2. Experimental

2.1 Experimental setup

An electron beam generator, which we used in our experiments, had a coaxial geometry. The scheme of the experimental setup is shown in Fig. 1. A discharge chamber (*1*) was a ceramic tube of length 21 cm with an inner diameter of 20 mm and a wall thickness of 2 mm. The dielectric constant of the ceramics was $\varepsilon = 4$. A copper foil (*2*) glued on the external surface of the tube served as one of the discharge electrodes. A grounded cylindrical anode (*3*) of length 18 cm was made of a steel grid with the 2×2-mm mesh. An accelerating gap between the inner surface of the ceramic tube and the anode was about of 1.5 mm. Copper inserts (*4*) were glued to the ends of the ceramic tube and served as a support for the anode grid and for gas pumping out and admission. At the ends of the inserts, quartz output windows (*5*) were placed at the Brewster angle to the tube axis. The discharge chamber was placed inside a plane–parallel resonator, which consisted of a highly reflecting mirror (*6*) and a semitransparent output mirror (*7*) with a reflection coefficient of 60 % at a wavelength of 2 μm. The laser output power was detected with an IMO-2 power meter (*8*). The output power distribution over the output aperture was measured with a PD25-02 photodiode with a sensitive-area diameter of 0.3 mm. The distribution of visible radiation over the chamber cross section was detected with a digital photographic camera. The discharge current was measured with a Rogowski loop (*9*) with a time resolution of 5 ns, which was determined by an oscilloscope (*10*). The experiments were performed with a He : Xe =30 : 1 mixture and in a pure helium.

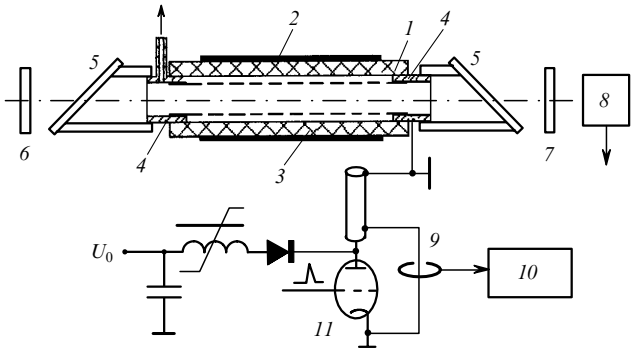

Figure 1. Scheme of the experimental setup: (*1*) discharge chamber; (*2*) copper foil; (*3*) anode grid; (*4*) copper inserts; (*5*) quartz plates; (*6*) gold mirror; (*7*) dielectric mirror; (*8*) IMO-2 power meter; (*9*) Rogowski loop; (*10*) TDS-410A oscilloscope; (*11*) TGI1-100/8 thyratron.

The energy was stored in a capacitance formed by the discharge chamber wall and the anode grid. The chamber was charged with the help of a resonance circuit consisting of the chamber capacitance and a choke with a saturable core and an initial inductance of 20 H. Due to the presence of a D1008 diode, the charging voltage U_c of the chamber capacitance was equal to the doubled supply voltage. The discharge pulse repetition rates f were varied from 0.01 to 10 kHz, and the supply voltage was varied from 0 to 6 kV.

The chamber capacitance was discharged by a thyratron triggering. A discharge was ignited in the dielectric–anode gap. A part of the electrons accelerated in the cathode layer of this gap were injected into the region behind the anode in the direction of the camber axis and excited the working gas. The pulse repetition rate f was limited not by the discharge circuit but the time of thyratron deionisation. For the charging voltage $U_c = 5 - 6$ and 3 kV, the pulse repetition rate was 10 and 40 kHz, respectively.

2.2 Measurements of the discharge current and voltage across the accelerating gap

In the presence of a dielectric barrier it is impossible to measure directly the discharge current J_d and the voltage drop U across the accelerating gap. These quantities can be only calculated from the values of the current J_m measured with a Rogowski loop, the capacity C_c of chamber (*1*), the capacity C_e of foil (*2*) and anode grid (*3*) with a dielectric between them (Fig. 1), and the capacity C_v representing a sum of the capacities of electric cables and C_e. These capacities measured under our experimental conditions were $C_c = 210$ pF, $C_e = 45$ pF, and $C_v = 79$ pF.

Analysis of the equivalent electric circuit of the discharge yields the following relations between the observed current J_m and quantities U and J_d, which are valid if the capacitor C_v is completely discharged to the instant t_d of the discharge ignition.

For the instant of time before the discharge ignition ($t < t_d$), we have

$$U = (1 - C_e/C_c) \int_0^t J_m dt/C_v, \quad J_d = 0. \tag{1}$$

For the instant of time after the discharge ignition ($t > t_d$), we have

$$U = (1 - C_e/C_c) \int_0^{t_d} J_m dt/C_v - \int_{t_d}^{t} J_m dt/C_c,$$
$$J_d = \frac{J_m}{(1 - C_e/C_c)}. \tag{2}$$

The maximum voltage across the discharge gap is $U_{max} = U_c(1 - C_e/C_c)$, and the electric strength vector is directed from the anode to dielectric. Expressions (1) and (2) were used for interpretation of the experimental current oscillograms.

3. Experimental results

3.1 Electric characteristics of the discharge

Typical oscillograms of the voltage $U(t)$ across the accelerating gap and of the discharge current $J_d(t)$, as well as the time dependence of the output power $P(t)$ obtained for $U_c = 11.3$ kV and $f = 1$ kHz in the He : Xe = 30 : 1 laser mixture at the pressure $p = 7.4$ Torr are shown in Fig. 2. The time dependence of the output power was measured directly, while the voltage across the accelerating gap and the discharge current were calculated by expressions (1) and (2) from the oscillograms of the current J_m and the charging voltage U_c of the chamber. These expressions are valid if the capacitor C_v is completely discharged to the instant t_d of the discharge ignition. In this case, two half-waves are observed in the oscillogram of the current J_m.

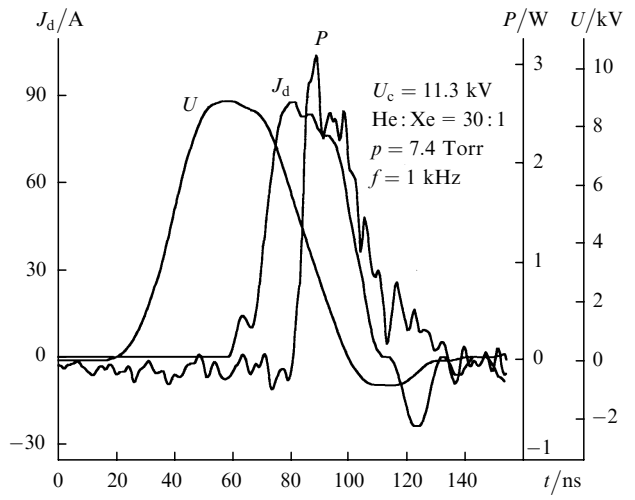

Figure 2. Oscillograms of the voltage U, discharge current J_d, and laser pulse P during the discharge in a laser mixture.

The first half-wave, which appears directly after the thyratron opening, is caused by the discharge of the capacitances of the connecting cable and a composite capacitor formed by the chamber and the accelerating gap. The second half-wave corresponds to the discharge in the dielectric (*1*)–anode (*3*) gap (Fig. 1). The time t_d was measured as the delay of the second half-wave with respect to the first one. The current observed under our experimental conditions was divided into two half-waves at $p < 9$ Torr. The maximum voltage across the accelerating gap was ~ 9 keV, which corresponds to $U_{max} \approx 0.8U_c$ (see section 2.2). The duration of the voltage-pulse front, which was determined by the discharge time of the capacitance of connecting cables, was ~ 50 ns. The maximum discharge current achieved ~ 87 A for the pulse base duration ~ 60 ns.

The voltage at the moment of the current maximum was ~ 5 keV (i.e., $\sim U_{max}/2$). This relation between the voltage across the accelerating gap at the moment of the current maximum and the maximum voltage is retained for any charging voltage U_c and discharge pulse repetition rates over the entire range from 10 Hz to 10 kHz. For $p > 9$ Torr, the half-waves in the oscillogram of the current coincided, while for $p > 30$ Torr, the discharge was ignited at the leading edge of the applied voltage pulse, which did not allow us to determine the discharge current and voltage across the discharge gap from the measured current J_{max}.

The oscillograms of the voltage U across the discharge gap and of the discharge current presented J_d in Fig. 2 can be used only as estimates because their calculations involve inevitable errors caused by the smoothing of noises in the oscillogram of the measured current J_m and errors of the numerical integration.

3.2 Visible emission of a gas

Fig. 3 shows the time-integrated exposures of visible emission excited by a fast-electron beam in a laser chamber at the discharge voltage $U_0 = 5$ kV and $f = 1$ kHz and different pressures of the working mixture. One can see that electrons excite the laser mixture at $p = 28$ Torr and helium at $p = 56$ Torr at a distance of ~ 5 mm from the grid. As the pressure is decreased, the diameter of a dark region at the central part of the chamber decreases, and the distribution of the emission intensity over the chamber diameter becomes homogeneous. At higher pressures, only a luminous strip is observed between the chamber wall and the grid anode, which corresponds to the discharge in the accelerating gap. Note that the discharge in the accelerating gap persists when pressure is increased up to 740 Torr both in helium and in the He–Xe mixture.

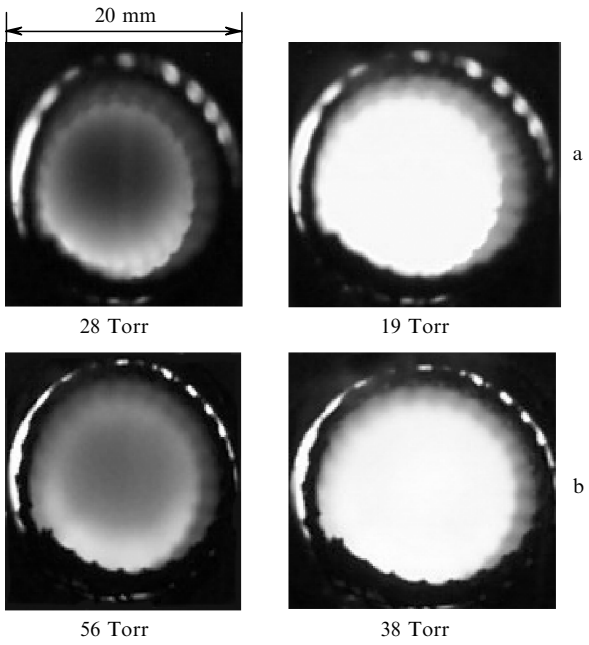

Figure 3. Emission of the He : Xe = 30 : 1 mixture (a) and He (b) excited by the electron beam at different pressures.

3.3 Parameters of the Xe laser

We studied the parameters of the laser without gas circulation. The working mixture was prepared directly in a working chamber before each series of experiments. The laser cell was evacuated down to $\sim 10^{-2}$ Torr and then was filled with xenon at a pressure of 10 Torr and helium at a partial pressure of 300 Torr. This mixture was evacuated to obtain the required pressure.

For a charging voltage of $5 - 6$ keV and a pulse repetition rate of up to 10 kHz, lasing was observed in the pressure range from 5 to 30 Torr. The average output power almost did not change during ~ 20 min after the discharge ignition. Then, the output power gradually decreased due to the contamination of the working mixture caused by the presence of many glued joints in the laser cell. Lasing ceased completely approximately after 1 h of the continuous operation of the laser at $f = 1$ kHz. A typical oscillogram of the output power $P(t)$ is shown in Fig. 2.

The best results were obtained for the mixture pressure $p = 18$ Torr and the maximum voltage across the discharge gap $U_{max} = 4.8$ kV. The dependence of the average output power P on the discharge pulse repetition rate under these conditions is shown in Fig. 4. One can see that the average power increases linearly with the pulse repetition rate. For the maximum pulse repetition rate $f = 10$ kHz, which was limited by the condition of a stable operation of the thyratron, the output power was 2.2 mW and the peak

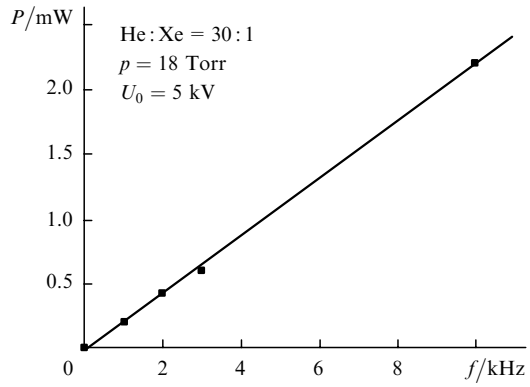

Figure 4. Dependence of the average laser output power P on the discharge pulse repetition rate.

output power was ~ 15 W. The distribution of the average output power over the laser aperture was virtually constant.

4. Discussion of results

To excite a gas efficiently by fast electrons using an open discharge as an electron-beam generator, one should decide two problems.

First, a stable discharge should be obtained in the accelerating gap. Here, we achieved this with the help of a barrier discharge, which remained stable under our conditions, as mentioned above, at gas pressures up to the atmospheric pressure. This result is very important because it demonstrates the possibility of producing an electron beam at gas pressures, which at least are an order of magnitude higher than maximum pressures achieved in the open discharge with metal electrodes [3–5].

Second, it is necessary to provide efficient excitation of the active medium over the entire chamber length by the electrons accelerated in the open discharge (the channel length in our experiments was ~ 1 cm).

The mean free path R of kiloelectronvolt electrons can be estimated from the known expression [11, 12]

$$R = 2.4 \times 10^{-6} \frac{E^2}{\rho}, \tag{3}$$

where R is the electron mean free path in a substance in cm; E is the electron energy in keV; and ρ is the substance density in g cm^{-3}. For helium, expression (3) takes the form

$$pR = 10E^2, \tag{4}$$

and for the laser He : Xe = 30 : 1 mixture studied by us, it has the form

$$pR = 5E^2, \tag{5}$$

where p is the gas pressure in Torr. One can see from expressions (4) and (5) that the electron mean free path in helium is two times greater than that in the laser mixture, the gas pressure and the initial energy of the electron beam being the same. This explains the similarity of the spatial distributions of gas emission in Fig. 3, which were obtained for the same electric parameters of the discharge but at the helium pressure that was two times higher than the pressure of the laser mixture.

Consider the conditions of the optimal energy input for the laser mixture studied by us. A decrease in the gas pressure at a fixed discharge voltage results in an increase in the mean free path of fast electrons and in a more homogeneous excitation of the laser chamber volume only up to a certain limit. When the mean free path R becomes greater than the chamber diameter D, a part of the electron-beam energy leaves the pump region and falls on the laser wall. Therefore, the condition of the optimal energy input is equivalent to equality (5), where $R \sim D$.

Let us estimate the average energy E of the fast-electron beam in our experiments. It follows from data [5] and our preliminary experiments that the shape of the current pulse of fast electrons completely reproduces the current pulse shape in the accelerating gap. The data presented in section 3.1 show that the voltage across the discharge gap at the moment of the current maximum is half the maximum voltage $U_{\max}$. Therefore, we can assume that most fast electrons have the energy $E \sim U_{\max}/2$, i.e., the condition of the optimal pump is

$$pD \sim 5(U_{\max}/2)^2. \tag{6}$$

Let us determine the pressure of the laser mixture that is optimal from the point of view of the spatial homogeneity and the loss of the electron energy and can be expected in experiments described in section 3.3. The substitution of $D \sim 2$ cm and $U_{\max} = 4.8$ kV into expression (6) yields $p_{\text{opt}} \sim 14.5$ Torr. Taking into account that these estimates are approximate, the obtained value is in good agreement with the experimental value equal to 18 Torr.

5. Conclusions

Therefore, we have confirmed experimentally the possibility of pulsed excitation of a dense gas by a broad-aperture electron beam injected from a barrier discharge. We have demonstrated the efficient excitation of visible emission and IR lasing at the xenon transitions. We have found that the barrier discharge of area ~ 100 cm^2 in a short gap (~ 1.5 mm) was stable at pressures of inert gasses and their mixtures up to the atmospheric pressure. The latter circumstance opens up the possibilities for a further many-parametric optimisation of the excitation conditions (frequency and voltage on the electron generator, dielectric-barrier material, composition and pressure of gases, geometry of the excitation chamber and the beam generator).

It is obvious that the electron-beam generator developed by us can be used both in the laser and plasma technologies.

Acknowledgements. This work was partially supported by the 'Integration' program (Fundamental Optics and Spectroscopy Educational and Scientific Center), the Russian Foundation for Basic Research (Grant No. 02-02-81008), and NATO (Grant No. 978204).

References

1. Basov N.G., Belenov E.M., Danilychev V.A., et al. *Pis'ma Zh. Eksp. Teor. Fiz.*, **20**, 421 (1971).
2. Zav'yalov M.A., Kreindel' Yu.E., Novikov A.A., et al. *Plazmennye protsessy v tekhnologicheskikh elektronnykh pushkakh*

(Plasma Processes in Industrial Electron Guns) (Moscow: Energoatomizdat, 1989).
3. Bokhan P.A., Zakrevskii D.E. *Pis'ma Zh. Tekh. Fiz.*, **28**, 74 (2002).
4. Sorokin A.Z. *Zh. Tekh. Fiz.*, **68** (3), 33 (1998).
5. Kolbychev G.V., Samyshkin E.A. *Kvantovaya Elektron.*, **10**, 437 (1983) [*Sov. J. Quantum Electron.,* **13**, 249 (1983)].
6. Ulrich A., Niebl C., Tomizawa H., et al. *J. Appl. Phys.,* **86**, 3525 (1999).
7. Azarov A.V., Mit'ko S.V., Ochkin V.N., Vitteman V.Ya. *Abstract of Papers, XXVII Zvenigorodskaya konf. po fizike plazmy i UTS* (XXVII Zvenigorod Conference on Plasma Physics and CTF) (Zvenigorod, 2000) p. 236.
8. Akishev Yu.S., Dyatko N.A., Napartovich A.P., Peretyat'ko P.I. *Zh. Tekh. Fiz.*, **59**, 512 (1998).
9. Ilyukhin B.I., Ochkin V.N., Tskhai S.N., et al. *Kvantovaya Elektron.*, **25**, 512 (1998) [*Quantum Electron.*, **28**, 497 (1998)].
10. Korolev V.S., Mal'tsev A.N. *Izv. Vyssh. Uchebn. Zaved., Ser. Fiz.*, (2), 7 (1992).
11. Curie M. *Radioaktivnost'* (Radioactivity) (Moscow: OGIZ, 1947).
12. Huddlestone R., Leonard S. (Eds) *Plasma Diagnostics* (Moscow: Mir, 1967).